CDF Results on Diffraction

Christina Mesropian[1]

[1] *on behalf of the CDF collaboration*
The Rockefeller University
1230 York Avenue, New York, NY, USA

We report results on diffraction obtained by the CDF collaboration in $p\bar{p}$ collisions at the Fermilab Tevatron collider at $\sqrt{s} = 1.96\,\text{TeV}$. The single diffractive dissociation processes such as diffractive dijet, W and Z productions are discussed. We also present results on double diffractive dissociation for central gap production. The first experimental observation of exclusive dijets is presented.

1 Introduction

Diffractive reactions, which constitute a substantial fraction of the total cross section in hadron-hadron scattering, can be described in terms of the *pomeron* exchange, hypothetical object with the quantum numbers of the vacuum. The experimental signatures of the diffraction consist in particular kinematic configurations of the final states: presence of non-exponentially suppressed large rapidity gaps and/or presence of the intact leading particles. The diffractive processes became an important tool in understanding many interesting aspects of QCD such as low-x structure of the proton, behaviour of QCD in the high density regime. Recently, a lot of attention was drawn to the possibility of discovering diffractively produced Higgs boson at the Large Hadron Collider (LHC). CDF collaboration contributed extensively [1]-[9] to significant progress in understanding diffraction by studying wide variety of diffractive processes at three different centre-of-mass energies: 630 GeV, 1800 GeV, Run I of Tevatron, and 1960 GeV - Run II. Some of the important results include the observation of the QCD factorisation breakdown in hard single diffractive processes, discovery of large rapidity gaps between two jets, study of diffractive structure function in double pomeron exchange dijet events.

2 CDF II Detector

The identification of diffractive events requires either tagging of the leading particle or observation of a rapidity gap, thus the forward detectors are very important for the implementation of a diffractive program. The schematic layout of CDF II detector is presented in Fig. 1. The Forward Detectors include the Roman Pot fiber tracker Spectrometer (RPS) used to select events with a leading $\bar{p}$, the Beam Shower Counters (BSCs), covering the pseudorapidity range $5.5 <| \eta |< 7.5$, detecting particles travelling in either direction from the interaction point along the beam-pipe, and the Miniplug Calorimeters (MP) [10] measuring energy and lateral position of electromagnetic and hadronic showers in the pseudorapidity region of $3.5 <| \eta |< 5.1$.

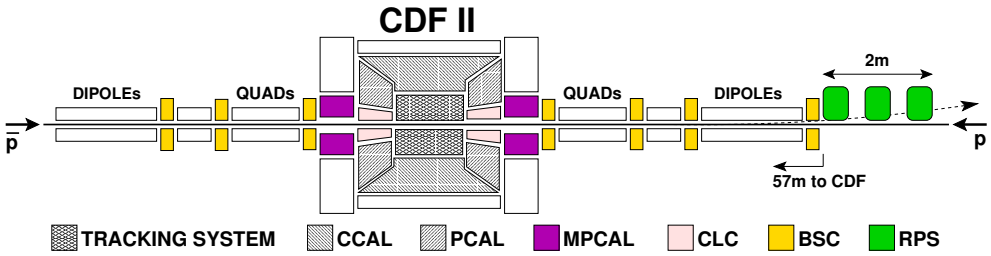

Figure 1: Schematic drawing of the CDF II detector.

3 Single Diffractive Dissociation

The signature of single diffractive (SD) dissociation at the Tevatron is either forward rapidity gap along the direction of one of the initial particles, or a presence of leading particle, antiproton, with $\xi < 0.1$. The process $\bar{p}p \to \bar{p}X$, which can be described by assuming that a pomeron is emitted by the incident antiproton and undergoes a hard scattering with the proton, is an ideal reaction to study the partonic content of the pomeron, and the diffractive structure function.

3.1 Diffractive Dijet Production

One of the single diffractive processes studied during Run I was the diffractive dijet production [6]. We compared two samples of dijet events, diffractive, triggered by the presence of intact antiproton detected in the RPS, and non-diffractive (ND). By taking the ratio of SD dijet rates to ND, which in a good approximation is the ratio of the diffractive to the known proton structure function, the diffractive structure function can be extracted. Our studies of the diffractive structure function were continued in Run II. One of the major challenges in diffractive studies during Run II is the presence of multiple $p\bar{p}$ interactions, which by overlapping with the diffractive event spoil signature characteristics of those, such as rapidity gaps. The rejection of *overlaps* was done by reconstructing ξ from the calorimeter towers, and considering only $\xi^{cal} < 0.1$, thus rejecting overlap events which have high ξ^{cal} values as a result of having more energy than just the diffractive interactions.

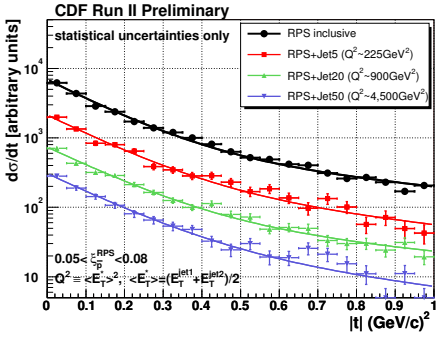

Figure 2: t distributions in soft and hard SD events for different Q^2 ranges.

We extended our results from Run I by studying $310\,\mathrm{pb}^{-1}$ SD data sample to examine the Q^2 dependence of the structure function up to $10^4\,\mathrm{GeV}^2$, where Q^2 is defined as an average value of mean dijet E_T. No appreciable Q^2 dependence was observed. We also studied the t distribution in single diffractive dijet events up to $Q^2 \sim 4500\,\mathrm{GeV}^2$, and no Q^2 dependence of the shape of the t distribution was observed, see Fig. 2.

3.2 Diffractive W, Z Production

The diffractive W/Z production is an important process for probing the quark content of the pomeron, since to leading order, the W/Z is produced through a quark, while the gluon associated production is suppressed by a factor of α_S and can be identified by an additional jet.

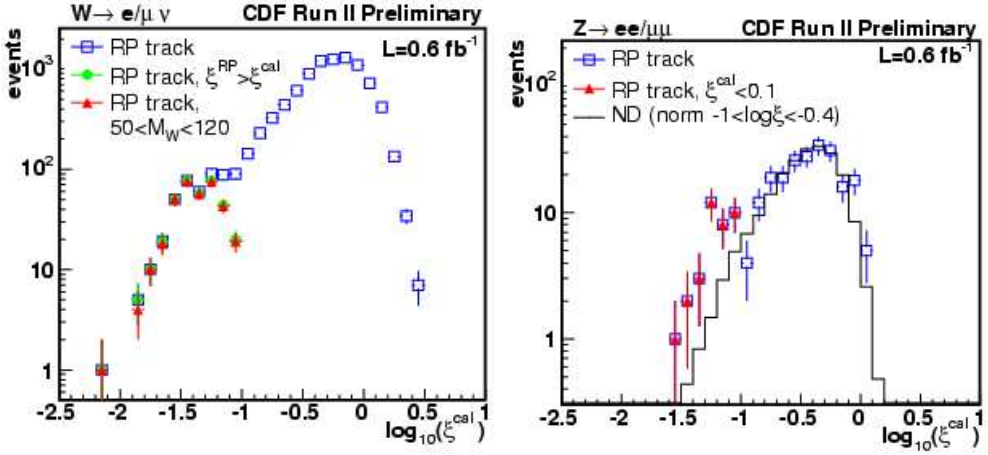

Figure 3: Calorimeter ξ distribution in W (left) and Z (right) events with a RPS track.

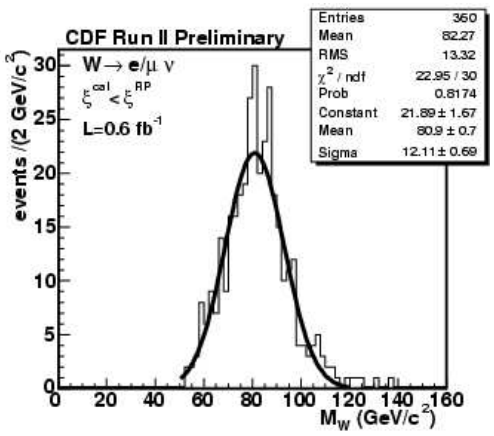

Figure 4: Reconstructed W mass in diffractive W candidate events.

In Run II, we developed a method that completely reconstructs W kinematics. The events are selected by utilising "intact leading antiproton" signature of the diffractive event. The RP spectrometer allows very precise ξ measurement, eliminating the problem of *gap survival probability*. The presence of a hit in the RPS trigger counters and a RPS reconstructed track with $0.03 < \xi < 0.1$ and $|t| < 1\,\mathrm{GeV}^2$ is required. The novel feature of the analysis, the determination of the full kinematics of the $W \to l\nu$ decay, is made possible by obtaining the neutrino ${E_T}^{\nu}$ from the missing E_T, $\not\!\!E_T$, and η_ν from the formula $\xi^{RPS} - \xi^{cal} = \frac{\not\!\!E_T}{\sqrt{s}} e^{-\eta_\nu}$, where ξ^{RPS} is true ξ measured in RPS and $\xi^{cal} = \sum_{i(towers)} (E_T^i/\sqrt{s}) exp(-\eta^i)$. Since we expect $\xi^{cal} < \xi^{RPS}$, we impose this requirement to remove overlap events to ensure that Ws were produced diffractively. Figures 3a,b show ξ^{cal} distributions for W and Z events with a RPS track. Figure 4 shows reconstructed W mass in diffractive W candidates. The requirements for W/Z selection are following: ${E_T}^l > 25\,\mathrm{GeV}$, $40 < M_T^W < 120\,\mathrm{GeV}$, $66 < M^Z < 116\,\mathrm{GeV}$, and $z-$vertex coordinate $z_{vtx} < 60\,\mathrm{cm}$. The fractions of diffractive W and Z events are measured to

be $[0.97 \pm 0.05(stat.) \pm 0.11(syst.)]\%$ and $[0.85 \pm 0.20(stat.) \pm 0.11(syst.)]\%$ for the kinematic range $0.03 < \xi < 0.10$ and $|t| < 1\,\mathrm{GeV}^2$. The measured diffractive W fraction is consistent with the Run I CDF result when corrected for the ξ and t range.

4 Double Diffractive Dissociation

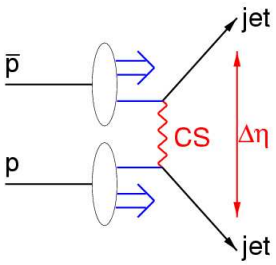

Figure 5: Schematic diagram of an event with a rapidity gap between jets produced in $p\bar{p}$ collisions.

Double diffractive (DD) dissociation is the process in which two colliding hadrons dissociate into clusters of particles (jets in case of hard DD dissociation) producing events with a large non-exponentially suppressed central pseudo-rapidity gap, see Fig. 5. Events with pseudorapidity gaps are presumed to be due to the exchange across the gap of a colour singlet (CS) object, *pomeron*, with vacuum quantum numbers. The dependence of the gap fraction on the width and on the position of the centre of the gap, $\Delta\eta^{gap}$ and ${\eta_c}^{gap}$, and the jet characteristics of the event are of great interest, as they allow testing different theoretical models. Measurements of DD have been performed for hard and soft diffraction processes [1, 4, 5, 8] for $p\bar{p}$ collisions at $\sqrt{s} = 630$ and 1800 GeV by the CDF collaboration. The extended rapidity coverage provided by the MP calorimeters ($3.5 < |\eta| < 5.1$) makes CDF II a powerful detector for hard DD studies, as it provides up to 8 units of η between jets for jets in the MPs. Using this data sample, we select events with two jets in the MPs with $E_T > 2\,\mathrm{GeV}$, $3.5 < |\eta^{jet}| < 5.1$, and $\eta_1\eta_2 < 0$. The E_T cut is designed to maximise the jet signal while minimising the effect of energy deposited by single particles and misidentified jets. We use this data sample to study

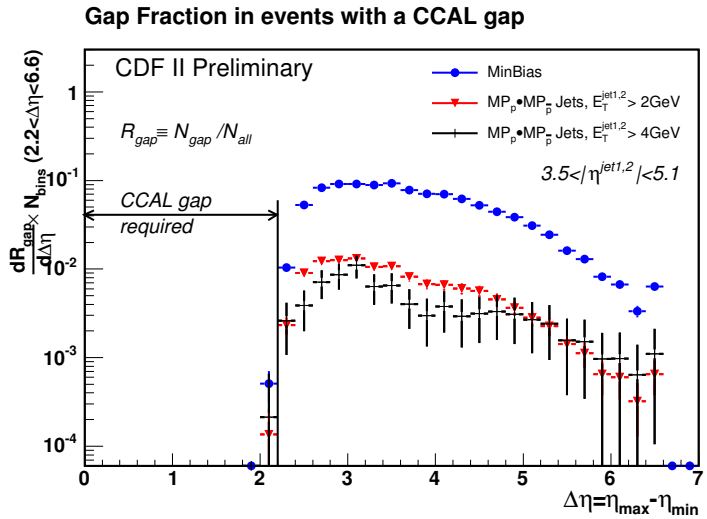

Figure 6: The distribution of the gap fraction $R_{gap} = N_{gap}/N_{all}$ vs. $\Delta\eta = \eta_{max} - \eta_{min}$ for min-bias and MiniPlug jet events of $E_T^{jet1,2} > 2\,\mathrm{GeV}$ and $E_T^{jet1,2} > 4\,\mathrm{GeV}$.

the dependence of the gap fraction on the width of the gap in "hard" and "soft" DD production. For this aspect of our analysis we use a definition of rapidity gap similar to that of our Run I study [8], where the rapidity gap variable, $\Delta\eta$, is defined as $\Delta\eta = \eta_{max} - \eta_{min}$, where η_{max} is the pseudorapidity of the particle (tower) closest to $\eta = 0$ in the proton direction and η_{min} is the pseudorapidity of the particle closest to the $\bar{p}$ direction. For events with gaps which overlap $\eta = 0$ these are effectively the edges of the rapidity gap. The data sample mentioned above is used to study "hard" diffraction production, where a hard structure (jet) is present in the event. "Soft" diffractive production is analyzed by examining low luminosity data collected with a min-bias trigger. Fig. 6 shows a comparison of the gap fraction, as a function of $\Delta\eta$, between "hard" and "soft" DD production when a rapidity gap is required within $-1.1 < \eta < 1.1$.

This comparison is relatively free of systematic uncertainties, as detector and beam related effects cancel out. The distributions are similar in shape, demonstrating that the gap fraction decreases with increasing $\Delta\eta$ for both "hard" and "soft" DD productions.

5 Exclusive Production

One of a very interesting topics of study at CDF is the central exclusive production. In leading order QCD such exclusive processes can occur through exchange of a colour-singlet two gluon system between nucleons, leaving large rapidity gaps in forward regions. One of the gluons participates in a hard interaction and additional screening gluon is exchanged to cancel the colour of the interacting gluons, allowing the leading hadrons to stay intact. This is also a special case of dijet/diphoton production in Double Pomeron Exchange (DPE), $p + \bar{p} \rightarrow p + X + \bar{p}$. Several different heavy systems X can be considered, but the main motivation for these studies is to use the process $p+\bar{p} \rightarrow p+H+\bar{p}$, see Fig. 7(a), to discover Higgs boson at the LHC. Although the cross section for the exclusive Higgs production is too small to be observed at the Tevatron, several processes mediated by the same mechanism but with the higher production rates can be studied to check theoretical predictions. Fig. 7(b-d) shows processes corresponding to studies in exclusive physics at the Tevatron: exclusive dijet, χ_c meson, and diphoton productions.The last two final states are discussed by M. Albrow and J. Pinfold in these proceedings.

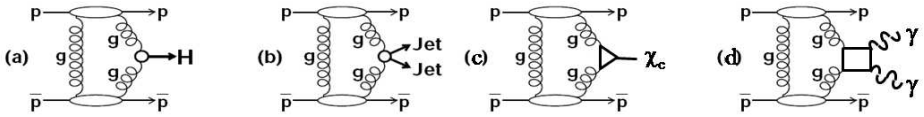

Figure 7: Diagrams of exclusive production of (a) Higgs boson, (b) dijet, (c) χ_c, and (d) a photon-photon pair.

5.1 Exclusive Dijet Production

The exclusive dijet production was first studied by CDF in Run I data and the limit of $\sigma_{excl} < 3.7\,\text{nb}$ (95% CL) was placed [11]. The data sample of $313\,\text{pb}^{-1}$ for the exclusive dijet production was collected in Run II with the dedicated trigger requiring a BSC gap on the proton side in the addition to the requirement for the leading anti-proton in the RPS and at least one calorimeter tower with $E_T > 5\,\text{GeV}$. The events in data sample also passed

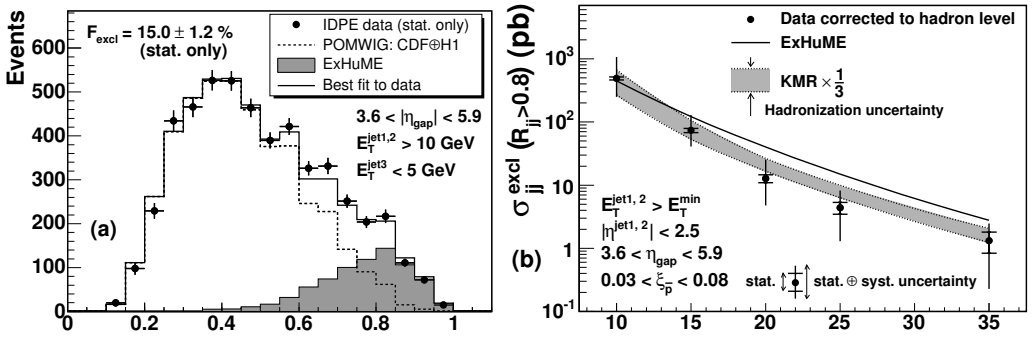

Figure 8: Dijet mass fraction in data (points), POMWIG MC and exclusive dijet (shaded histogram) MC events (left); Exclusive dijet cross sections for events with two jets and with $R_{jj} > 0.8$ (right).

the offline requirement of additional gap in MP on the proton-side. The exclusive signal is extracted using the dijet mass fraction method: from the energies and momenta of the jets in an event, the ratio $R_{jj} \equiv M_{jj}/M_X$ of the dijet mass M_{jj} to the total mass M_X of the final state (excluding the p and $\bar{p}$) is formed and used to discriminate between the signal of exclusive dijets, expected to appear at $R_{jj} = 1$, and the background of inclusive DPE dijets, expected to have a continuous distribution concentrated at lower R_{jj} values. Because of smearing effects in the measurement of ${E_T}^{jet}$ and jet and gluon radiation from the jets, the exclusive dijet peak is broadened and shifts to lower R_{jj} values. The exclusive signal is obtained by a fit of the R_{jj} distribution to expected signal and background shapes generated by Monte Carlo (MC) simulations. The data clearly show an excess at high R_{jj}, see Fig. 8 (left) over the non-DPE background events and inclusive DPE predictions obtained from POMWIG MC. The shape of excess is well described by exclusive dijet MC based on two models (ExHuME [12], DPEMC [13]); however, the measured cross section [14], see Fig. 8 (right), disfavours DPEMC. Predictions [15] are found to be consistent with data within its factor of 3 uncertainty. The results could also be checked with an event sample of heavy quark flavor dijets, for which exclusive production is expected to be suppressed in LO QCD by the $J_z = 0$ selection rule of the hard scattered digluon system, where J_z is the projection of the total angular momentum of the system along the beam direction. Fig. 9 shows comparison between exclusive dijet results obtained with MC-based method and the data based suppression of the exclusive heavy flavor to inclusive dijet production rates. The results are consistent with each other.

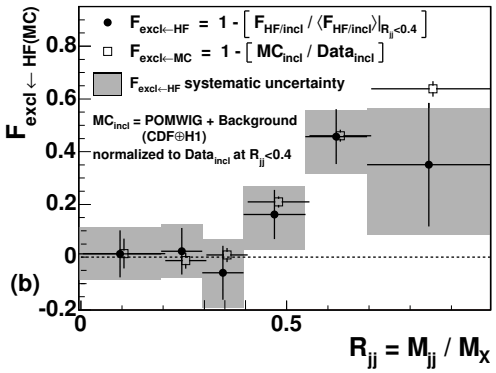

Figure 9: Measured ration F_{HF} (filled circles) of heavy flavor jets to all inclusive jets and the exclusive dijet ratio F_{excl} (open squares) obtained by comparison between inclusive dijet events and POMWIG MC.

6 Conclusions

The CDF collaboration continues the long-standing extensive program of diffractive studies. Our Run II results include measurements of diffractive structure function and t distribution from single diffractive dijet production, the measurement of diffractive W/Z production using Roman Pot Spectrometers, and study of double diffractive processes in events with a central rapidity gap. In addition, the first observation of exclusive dijet production by CDF provides an important calibration for the predictions of the exclusive Higgs production at the LHC.

Acknowledgements

I would like to thank the organisers of 13th International Conference on Elastic & Diffractive Scattering for warm hospitality and for an exciting conference.

References

[1] F. Abe *et al.,* Phys.Rev.Lett. **74**, 855 (1995).

[2] F. Abe *et al.,* Phys.Rev.Lett. **78**, 2698 (1997).

[3] F. Abe *et al.,* Phys.Rev.Lett. **79**, 2636 (1997).

[4] F. Abe *et al.,* Phys.Rev.Lett. **80**, 1156 (1998).

[5] F. Abe *et al.,* Phys.Rev.Lett. **81**, 5278 (1998).

[6] T. Affolder *et al.,* Phys.Rev.Lett. **84**, 5043 (2000).

[7] T. Affolder *et al.,* Phys.Rev.Lett. **85**, 4215 (2000).

[8] T. Affolder *et al.,* Phys.Rev.Lett. **87**, 141802-1 (2001).

[9] T. Affolder *et al.,* Phys.Rev.Lett. **87**, 241802-1 (2001).

[10] K. Goulianos *et al.,* Nucl.Instrum.Methods A **518**, 24 (2004).

[11] T. Affolder *et al.,* Phys.Rev.Lett. **85**, 4215 (2000).

[12] J. Monk and A. Pilkington, Comput.Phys.Commun. **175**, 232 (2006).

[13] M. Boonekamp and T. Kuss, Comput.Phys. Commun. **167**, 217 (2005).

[14] T. Aaltonen *et al.,* Phys.Rev. D **77** 052004 (2008).

[15] V.A. Khoze *et al.,* Eur. Phys.J. C **14**, 525 (2000); V.A. Khoze *et al.,* arXiv:0705.2314.

[16] A.D. Martin *et al.*, Eur. Phys. J. **C39** 155 (2005).